1 **Title: p63 cooperates with CTCF to modulate chromatin architecture in skin keratinocytes**

2 Jieqiong Qu[1#], Guoqiang Yi[2#], Huiqing Zhou[1, 3]*

3

4 **Affiliations:**

5 [1]Department of Molecular Developmental Biology, Faculty of Science, Radboud Institute for

6 Molecular Life Sciences, Radboud University, Nijmegen, the Netherlands

7 [2]Department of Molecular Biology, Faculty of Science, Radboud Institute for Molecular Life Sciences,

8 Radboud University, Nijmegen, the Netherlands

9 [3]Department of Human Genetics, Radboud university medical centre, Nijmegen, the Netherlands

10 * Correspondence: Huiqing Zhou

11 [#] These authors contribute to the manuscript equally.

12

13

14 E-mail address of all authors:

15 Jieqiong Qu: jqu@science.ru.nl

16 Guoqiang Yi: guoqiang.yi@science.ru.nl

17 Huiqing Zhou: j.zhou@science.ru.nl; jo.zhou@radboudumc.nl

18

19

20

1   **Abstract**

2   The transcription factor p63 regulates epidermal genes and the enhancer landscape in skin

3   keratinocytes. Its molecular function in controlling the chromatin structure is however not yet

4   completely understood. Here we integrated multi-omics profiles, including the transcriptome,

5   transcription factor DNA-binding and chromatin accessibility, in skin keratinocytes isolated from EEC

6   syndrome patients carrying p63 mutations, to examine the role of p63 in shaping the chromatin

7   architecture. We found decreased chromatin accessibility in p63- and CTCF-bound open chromatin

8   regions that potentially contributed to gene deregulation in mutant keratinocytes. Cooperation of

9   p63 and CTCF seemed to assist chromatin interactions between p63-bound enhancers and gene

10   promoters in skin keratinocytes. Our study suggests an intriguing model where cell type-specific

11   transcription factors such as p63 cooperate with the genome organizer CTCF in the three-

12   dimensional chromatin space to regulate the transcription program important for the proper cell

13   identity.

14

15

1 **Introduction**

2 Skin development and homeostasis requires tightly regulated epidermal keratinocyte proliferation,

3 differentiation and apoptosis, and these processes are governed by cooperation of cis-regulatory

4 elements, transcription factors (TFs), chromatin accessibility as well as higher-order chromatin

5 organisation [1-5]. The TF p63 is a key regulator of epidermal development. At the molecular level,

6 p63 regulates a large number of genes , for example, p21 (*CDKN1A*) in cell cycle arrest [6], Fras1 in

7 maintaining basement membrane integrity [7] and key genes such as keratins, filaggrin, and loricrin

8 required for epidermal morphogenesis and differentiation [1, 8]. Furthermore, p63 directly regulates

9 chromatin factors, Satb1, Lsh, and Brg1, to control the chromatin remodelling during epidermis

10 development [9-11]. Recent studies showed that p63 exerts a crucial role in establishing the

11 enhancer landscape [4, 5, 12, 13]. Through active enhancers, p63 cooperates with its co-regulating

12 TFs to modulate local transcriptional program required for epidermal homeostasis [4].

13 In human, heterozygous mutations of *TP63* encoding p63 cause a spectrum of ectoderm-related

14 disorders [14]. For example, Ectrodactyly-Ectodermal Dysplasia-Cleft Lip/Palate (EEC) syndrome is

15 caused by point mutations located in the p63 DNA-binding domain, and manifests ectodermal

16 dysplasia with defects in the epidermis and epidermal related appendages, limb malformation and

17 cleft lip/palate. Five hotspot mutations affecting amino acids, R204, R227, R279, R280 and R304,

18 cover approximately 90% of the all EEC syndrome cases [15]. Our previous study showed that

19 mutant p63 resulted in a genome-wide redistribution of enhancers in keratinocytes established from

20 EEC patients [13]. Consistently, the gene network analysis identified a significant co-expression gene

21 module of 'nucleosome assembly', implying a less-organized chromatin structure in EEC syndrome

22 keratinocytes [13]. How mutant p63 affects the chromatin structure is however not yet clear.

23 In this study, we characterized the chromatin accessibility using ATAC-seq in keratinocytes

24 established from EEC patients carrying p63 mutations, in comparison with control keratinocytes. A

25 clear difference in chromatin accessibility that correlated with the transcriptional dynamics was

26 detected. Unexpectedly, strong enrichment of CTCF binding siteswere observed at control-specific

27 open chromatin regions. By combining published promoter Capture Hi-C seq data, we found that

28 CTCF and p63 were cooperatively involved in DNA loops to regulate epidermal genes. Our findings

29 provide new insights into the coordinated regulatory role of CTCF and p63 in chromatin interactions

30 in epidermal keratinocytes.

31

32

1   **Results**

2   **Differential chromatin accessibility between control and p63 mutant keratinocytes**

3   We performed Assay for Transposase-Accessible Chromatin with high-throughput sequencing (ATAC-

4   seq) to characterize the accessible genome as well as the nucleosome position in both control and

5   p63 mutant keratinocytes at the proliferation stage. Two replicas of ATAC-seq analyses showed high

6   correlation (Figure 1A), indicating high reproducibility. The principle component analysis (PCA) plot

7   based on the chromatin accessibility displayed a clear separation between control and p63 mutant

8   keratinocytes (Figure 1B), which is highly consistent with results from gene expression profiles

9   (Figure 1B). The PCA analysis also showed that the genome accessibility of the two p63 mutant lines

10   (R204W and R304W) are similar, as they are close on the PC1 axis that represents major variations.

11   As the goal of this work is to examine the difference between control and EEC mutant lines, these

12   two mutant lines were considered as one group, termed as p63 mutant keratinocytes, in the

13   following analyses.

14   Subsequently we identified the differential open chromatin regions (OCRs) marked by ATAC-seq

15   signals between control and p63 mutant keratinocytes. In total, there were 2,492 open chromatin

16   regions that showed higher signal in control keratinocytes, termed as control-specific open

17   chromatin regions (Ctr-OCRs); in parallel, there were 3,716 regions that showed higher signal in

18   mutant keratinocytes, termed as mutant-specific open chromatin regions (Mt-OCRs) (Figure 1C). As

19   expected, we found that differential OCRs were positively correlated with gene expression, when

20   they were assigned to the nearest differentially expressed (DE) genes (Figure 1C). Genes associated

21   with Ctr-OCRs were mainly involved in the regulation of 'cell cycle' (Figure 1D), e.g. *CDC7* (Figure 1E),

22   while genes nearby Mt-OCRs were mainly enriched in 'actin filament-based process' (Figure 1D), e.g.

23   *FAP* (Figure 1E).

24   **p63 and CTCF occupancy at Ctr-OCRs**

25   To identify the potential TFs involved in these differential OCRs, we first performed a comparative

26   motif analysis between control and p63 mutant keratinocytes using HOMER. Among the Ctr-OCRs,

27   we found that p63 motif is most enriched (Figure 2A), which is consistent with our previous finding

28   that loss of p63 binding resulted in decreased enhancers in p63 mutant keratinocytes [13].

29   Unexpectedly, the motif of CTCF that is a well-known genome organizer [16] was identified as the 2nd

30   highly enriched motif in the Ctr-OCRs. Among the Mt-OCRs, AP-1 motif family was most enriched

31   (Figure 2B), consistent with findings on gained enhancers in p63 mutant keratinocytes [13].

1   To validate our motif analysis result and explore the role of p63 in controlling Ctr-OCRs, we used

2   published p63 ChIP-seq data from our previous work [13]. In control keratinocytes, a total of 1,223

3   p63 binding sites (BSs) were covered by the 2,492 Ctr-OCRs, showing a significant overlap ($p < 0.001$).

4   When ATAC-seq and p63 ChIP-seq reads were mapped to the 1,223 p63-bound Ctr-OCRs, we found a

5   decrease of both chromatin accessibility and p63 binding signals at the p63-bound Ctr-OCRs in p63

6   mutant keratinocytes (Figure 2C).

7   To confirm the role of CTCF in Ctr-OCRs, we performed CTCF ChIP-seq in both control and p63

8   mutant keratinocytes. In total, we found 12,116 CTCF BSs, among which only 363 were differential in

9   CTCF binding between control and p63 mutant keratinocytes ($p < 0.05$), indicating that CTCF binding

10   is rather stable. In addition, among all putative CTCF BSs, we found 376 overlapped with the 2,492

11   Ctr-OCRs, which is statistically significant ($p < 0.001$). We then mapped ATAC-seq and CTCF ChIP-seq

12   reads to the 376 CTCF-bound Ctr-OCRs. As expected, decrease of ATAC-seq signals was observed at

13   the CTCF-bound Ctr-OCRs in p63 mutant keratinocytes. However, unexpectedly, there was no

14   significant change in CTCF binding signals at the CTCF-bound Ctr-OCRs in p63 mutant keratinocytes,

15   as compared to the control keratinocytes (Figure 2D). Another expected finding was that there is few

16   overlap (N=435) out of 45,350 p63 BSs and 12,116 CTCF BSs (Supplementary Figure 1A), although

17   both motifs were identified in Ctr-OCRs. Consistently, there was no visible CTCF binding signal at all

18   p63 BSs, and vice versa, no visible p63 binding at the CTCF BSs (Supplementary Figure 1B).

19   Consistently, we also observed decreased p63 binding and largely unchanged CTCF binding signal in

20   p63 mutant keratinocytes at the co-localized binding sites (Supplementary Figure 1C).

21   Subsequently, we analyzed the nucleosome positioning at p63-bound and CTCF-bound Ctr-OCRs by

22   mapping the distribution of ATAC-seq fragments centered on either p63 motif or CTCF motif (Figure

23   2E). In control keratinocytes, we found an enrichment of short fragments (< 150 bp) surrounding

24   both p63 motif and CTCF motif. The enrichment of such short reads clearly decreased in p63 mutant

25   keratinocytes (Figure 2E and Supplementary Figure 2). We also observed an enrichment of

26   fragments that had lengths slightly shorter than 200 bp which represent the stable flanking

27   nucleosomes in control keratinocytes. However, in p63 mutant keratinocytes, the approximate 200

28   bp length-fragments seemed to be less present (Supplementary Figure 2), indicating an altered

29   nucleosome organization.

30   Taken together, we observed decreased accessibility at p63-bound and CTCF-bound Ctr-OCRs in p63

31   mutant keratinocytes when compared to control keratinocytes. Notably, there was a clear decrease

32   of p63 binding at the p63-bound Ctr-OCRs whereas CTCF binding did not seem to be affected at the

33   CTCF-bound Ctr-OCRs in p63 mutant keratinocytes.

Characterization of p63-bound OCRs and CTCF-bound OCRs

We reasoned that the chromatin states and the genomic locations of these Ctr-OCRs might be informative to understand the difference between p63-bound and CTCF-bound Ctr-OCRs. To this end, we firstly analyzed the chromatin states (CSs) of all CTCF and p63 BSs with the combination of six histone marks from Roadmap project [17] (Figure 3A). We found that p63 bound to both promoters and enhancers marked by H3K27ac and H3K4me1, whereas CTCF was more enriched at promoters marked by H3K4me3 (Figure 3A and Supplementary Figure 3). We then performed analyses on the p63- and CTCF-bound Ctr-OCRs (Figure 3B). When comparing to all Ctr-OCRs, p63-bound Ctr-OCRs were overrepresented at enhancers (CSs 8, 9, and 11) while the majority of CTCF-bound Ctr-OCRs showed overrepresentation at promoter proximal regions (CSs 2 and 4, Figure 3B), consistent with all p63 and CTCF BSs.

Next, to analyze the localization of p63-bound and CTCF-bound Ctr-OCRs in regulatory chromatin interactions, we utilized the Promoter Capture Hi-C (PCHiC) data and TAD (topologically associating domain) regions from published HiC data in keratinocytes [18]. In the PCHiC, promoters were used as baits to capture the interacting genomic regions. In total, this PCHiC dataset captured 119,648 interactions, including 103,497 (86.5%) promoter-enhancer loops and 16,151 (13.5%) promoter-promoter loops (Figure 3C). As p63 plays a more prominent role at enhancers (Figure 3A) [4], we focused on promoter-enhancer loops. These loops had a median loop size of 250.9 kb (Figure 3D). Among the previously defined 1,223 p63-bound Ctr-OCRs (Figure 2C), 388 of them were located at the anchors of 1,674 loops, at either the promoter or the enhancer, and on average one p63-bound Ctr-OCR was connected by ~4.3 loops. Similarly, among the 376 CTCF-bound Ctr-OCRs (Figure 2D), 191 of them were located at the anchors of 1,093 loops; on average, one CTCF-bound Ctr-OCR was connected by ~5.7 loops. Therefore, CTCF-bound Ctr-OCRs at anchors were connected by more loops.

Furthermore, we found that CTCF-bound Ctr-OCRs located at loop anchors were more enriched for promoters (~ 4 fold) (Figure 3E), consistent with all CTCF BSs and all CTCF Ctr-OCRs. In contrast, p63-bound Ctr-OCRs associated with loops were enriched in both promoters and enhancers to a similar extent (Figure 3E), which is different from all p63 BSs and all p63-bound Ctr-OCRs that were only enriched at enhancers (Figure 3B). We also examined whether p63- and CTCF-bound Ctr-OCRs were localized at the TAD boundaries. As expected, CTCF-bound Ctr-OCRs showed ~2.5 fold enrichment for TAD boundaries, whereas p63-bound Ctr-OCRs were depleted of TAD boundaries (Figure 3E). Randomization by reshuffling genomic regions with same sizes did not show any enrichment in TAD boundaries, promoters or enhancers. As CTCF-bound Ctr-OCRs were enriched at the promoters and p63-bound Ctr-OCRs were enriched at both promoters and enhancers, it is plausible that p63-bound

1   enhancers interact with CTCF-bound promoters to regulate genes through DNA looping and a subset

2   of these loops may be affected by p63 mutations.

3   **p63 and CTCF mediate a subset of loops to regulate transcription**

4   To assess how p63 and CTCF cooperates via DNA looping to regulate gene expression, we performed

5   further analyses using previously published gene expression data [13] to examine the relation

6   between gene expression and DNA looping. In control keratinocytes, we defined highly expressed

7   genes by quartiles to four groups using their transcriptional levels (Q1-4, FPKM ≥ 1), and another

8   group with lowly expressed genes (Q0, FPKM < 1). We detected an increasing number of associated

9   loops with elevated gene expression levels (Figure 4A). This suggests that highly expressed genes

10   may be more indispensable of regulation through loops, which is line with previous study showing

11   multi-loop activation hubs at key regulatory genes [19]. Moreover, the differentially expressed genes

12   between control and p63 mutant keratinocytes (Figure 1B) were associated with significantly more

13   loops ($p < 0.001$) than all expressed genes (Figure 4B). We also performed the same analysis among

14   loops with either p63-bound or CTCF-bound Ctr-OCRs. Similar results were found, although in these

15   comparisons the difference was not significant, probably due to the low number of associated loops

16   (Figures 4C and D).

17   We then mapped 388 p63-bound and 191 CTCF-bound Ctr-OCRs which are located at loop anchors

18   to their target genes by identifying their interacting gene promoters located at anchors of the other

19   end of the loops. In some cases, Ctr-OCRs were located in promoters, and the associated genes were

20   considered as target genes. In total, 388 p63-bound Ctr-OCRs interacted with 304 gene promoters

21   while 191 CTCF-bound Ctr-OCRs interacted with 500 gene promoters through looping interactions,

22   indicating that on average a CTCF-bound Ctr-OCR is involved in the regulation of more genes than a

23   p63-bound Ctr-OCR. There was a significant ($p < 0.001$) overlap (N = 96) of genes that were

24   potentially regulated by p63- and CTCF-bound Ctr-OCRs (Figure 4E). These 96 genes represent genes

25   connected by the promoter-enhancer loops that were anchored by both p63-bound and CTCF-bound

26   Ctr-OCRs and that may be affected in p63 mutant keratinocytes. As the three-dimensional chromatin

27   landscape is relatively stable, we reasoned that the difference of the chromatin landscape in control

28   and p63 mutant keratinocytes may influence gene expression during keratinocyte differentiation

29   [18]. Therefore, we examined the expression of these 96 genes using previously reported differential

30   gene expression in control and p63 mutant keratinocytes during differentiation [13]. Indeed we

31   found that 39 of these 96 genes showed deregulation ($p < 0.001$). Notably many of the 96 genes

32   were involved in 'epidermal cell differentiation', e.g. *KRT5*, *KRT75*, and *B9D1* (Figure 4F).

1   Next, we dissected how p63-bound and CTCF-bound Ctr-OCRs at loop anchors co-regulated these 96

2   genes: whether p63-bound and CTCF-bound Ctr-OCRs were involved in the same or different

3   promoter-enhancer loops. We found that 60 genes were regulated by promoter-enhancer loops

4   where p63-bound and CTCF-bound Ctr-OCRs were both located at the anchors in the same loops,

5   although they may co-localized in different manner (Figure 4G). Among these 60 genes, 26 showed

6   differential expression between control and p63 mutant keratinocytes during differentiation, with

7   *PIGV* and *KRT5* shown as examples (Figures 4I and J). Among the loops associated with the 60 genes,

8   the case where p63-bound Ctr-OCR was located at one anchor while CTCF-bound Ctr-OCR was

9   located at the other anchor of the loop counted for 12.6% (Figure 4G, (1)). In the majority of the

10   cases, both p63-bound and CTCF-bound Ctr-OCRs were present either at the promoter (70.6%)

11   (Figure 4G, (2)) or at the enhancer (16.8%) (Figure 4G, (3)). Interestingly, for the rest 36 genes gene

12   promoters were connected with both p63-bound and CTCF-bound Ctr-OCRs from different loops

13   (Figure 4H), suggesting that enhancers occupied by p63-bound and CTCF-bound Ctr-OCRs can co-

14   regulate the same gene through different loops. Among these 36 genes, 13 were deregulated in p63

15   mutant keratinocytes during differentiation.

16

1 **Discussion**

2 Over the years, molecular understanding of p63 function in keratinocytes has led to the

3 identification of numerous target genes including chromatin factors [20-22] as well as of a solid role

4 of p63 in orchestrating the enhancer landscape [4, 5, 23]. However, whether p63 is involved in the

5 direct regulation of chromatin architecture is not known. In this study, we characterized the

6 chromatin accessibility with ATAC-seq in both control and EEC syndrome patient keratinocytes

7 carrying p63 mutations (R204W and R304W). Interestingly, we found decreased chromatin

8 accessibility in p63- and CTCF-bound open chromatin regions in mutant p63 keratinocytes. These

9 less accessible chromatin regions interact with epidermal gene promoters and potentially regulate

10 gene expression. Collectively, we proposed an unreported role of p63 ~~directly~~ cooperating with CTCF

11 in chromatin interactions.

12 It is envisaged that p63 is a key factor in skin keratinocytes [4, 5, 24]. Ample studies have shown that

13 the proper regulation of gene expression by p63 through the precise control of enhancers is

14 essential for maintaining the epidermal cell identity [4, 13, 25, 26]. It is equally important that p63

15 requires additional co-regulating TFs to regulate transcription. Several studies reported p63 co-

16 regulating TFs, e.g. AP1, AP2, STAT5, and RFX5 [20, 22, 23, 27], which are essential for the epidermal

17 gene expression in a temporal and spatial manner [4, 28]. Besides, p63 interacts with the chromatin

18 remodelling factor BAF1 to maintain the open chromatin regions [5] and with Dnmt3a to locate

19 enhancers [12]. In this study, we found that CTCF, a well-known TF maintaining the chromatin

20 architecture, is also a p63 co-regulating TF modulating a subset of chromatin loops. However, this

21 cooperation is probably not through direction protein-protein interactions but mainly bridging

22 enhancers and promoters, given the few overlap observed between p63 and CTCF BSs. It is known

23 that the majority of p63-bound regions are located in intergenic or intragenic regions (enhancers)

24 rather than promoters [22], and therefore how p63-bound enhancers interact with gene promoters

25 is an interesting question. Our current study provides the first line of evidence that the cooperation

26 with CTCF assists the looping of p63-bound enhancers to gene promoters.

27 The observation of the enriched CTCF motif in Ctr-OCRs detected in our ATAC-seq analyses was

28 somewhat unexpected. Our previous enhancer-centred analysis that focused on H3K27ac enriched

29 genomic regions did not capture CTCF motifs [4, 13], probably due to the fact that CTCF is more

30 enriched in open chromatin regions depleted of H3K27ac but enriched for H3K4me3 signal (Figure

31 3A and Supplementary Figure 3). Interestingly, detecting the CTCF motif in Ctr-OCRs in keratinocytes

32 is in line with the previous finding that the motif of YY1 was enriched in p63-bound sequences [27].

33 YY1 has been shown to co-localize with CTCF and stabilize chromatin looping [29, 30].

1. CTCF maintains the genome organization by occupying the boundaries of megabase-scale TADs, and

2. functions as an insulator to block enhancer-promoter interactions between different TADs [16]. Our

3. date showed that, in addition to demarcating TADs, CTCF mediates promoter-enhancer loops, often

4. located in promoter-proximal regions (Figure 3E), to facilitate the promoter-enhancer interactions

5. within one TAD. This is in line with the concept that a subpopulation of CTCF associates with the RNA

6. polymerase II (Pol II) protein complex to activate transcription [31]. It is likely that CTCF helps to

7. bridge the p63-bound enhancers to transcription start site-proximal regulatory elements and to

8. initiate transcription by interacting with Pol II, thus supporting a role of CTCF in facilitating contacts

9. between transcription regulatory sequences. This model has been demonstrated by the previous

10. work on the beta-globin locus [32]. To get a clearer picture, technologies that are similar to ChIA-PET

11. [33], such as HiChIP [34], would be useful to understand long-range contacts associated with CTCF or

12. p63 in skin keratinocytes.

13. The three-dimensional chromatin landscape is relatively stable once established in a specific cell

14. type, probably during cell commitment, and cell-type-specific looping structures mainly control the

15. accessibility of enhancers to their specific targets [35]. Recent studies showed that cell type-specific

16. TFs are involved in regulation of DNA looping in macrophage development, which shed light on the

17. role of cell type-specific TFs in regulating chromatin interactions [19]. Here we proposed that a

18. number of loci nearby epidermal genes were organized into a 'regulatory chromatin hub' within the

19. chromatin interactions mediated by CTCF in epidermal keratinocytes (Figure 5A). Such hubs contain

20. multiple connecting DNA loops that require not only CTCF binding that is rather static but also

21. binding of cell type-specific TFs (e.g. p63) for the transcriptional activity. In this model, cell type-

22. specific TFs may be essential to make the DNA loops active in transcription. This hypothesis is

23. consistent with our observation that unchanged CTCF binding signal but decreased accessibility in

24. the CTCF-bound Ctr-OCRs in p63 mutant keratinocytes (Figure 2D).

25. Moreover, our observations shed light on the chromatin-based mechanisms underlying EEC

26. syndrome caused p63 mutations. These EEC mutations, such as R204W and R304W, were shown to

27. disrupt p63 DNA binding, resulting in impaired transactivation activity and loss of epidermal cell

28. identity [13, 36, 37]. Our data suggest that deregulated function of DNA loops mediated by p63 and

29. CTCF represents an additional layer to the disease mechanism (Figure 5B). Given that CTCF binding

30. did not change, it is likely that the looping interactions are static, but the looping is no longer active

31. due to the absence of p63 binding (Figure 5B (1)). Therefore, the epidermal genes were down-

32. regulated and p63 mutant keratinocytes showed loss of epidermal cell identity [13]. On the other

33. hand, it is also possible that the loop ablation as a result of lost p63 binding leads to the decreased

1   accessibility at CTCF-bound promoters and deregulated gene expression in p63 mutant keratinocytes

2   (Figure 5B (2)). The latter scenario suggests p63 is the key factor determining the regulatory activity

3   of such promoter-enhancer interactions. Nevertheless, how p63 mutations affect the cooperation

4   between p63 and CTCF and gene expression is still unclear. Among the 96 genes with loops

5   connected by p63- and CTCF-bound Ctr-OCRs, only 39 of them were deregulated in p63 mutant

6   keratinocytes. It is possible that 'shadow enhancers' that are composed of clusters of enhancer and

7   contribute to robust gene transcription [38, 39], are involved in regulation of the 57 genes that are

8   not deregulated in mutant keratinocytes. Further experiments are required to test these hypotheses.

9   Taken together, our results highlight the cooperation of p63 and CTCF in mediating DNA loops as

10   well as gene regulation. These observations provide new insights into the general regulatory role of

11   chromatin looping which depends on the coordination of CTCF and cell type-specific TFs such as p63

12   in skin keratinocytes.

13

1 **Material and methods**

2 **Ethics statement**

3 All procedures for establishing and maintaining human primary keratinocytes were approved by the

4 ethical committee of the Radboud university medical center ("Commissie Mensgebonden Onderzoek

5 Arnhem-Nijmegen"). Informed consent was obtained from all donors of a skin biopsy.

6 **Human primary keratinocyte culture**

7 Primary keratinocytes were established previously from skin biopsies of three EEC syndrome

8 patients carrying heterozygous mutations in the p63 DNA-binding domain, R204W[40] and R304W

9 [37], as well as of non-EEC volunteers (Dombi23, referred to as control) [41]. R204W and R304W are

10 treated as a p63 mutant group for further analyses to minimize the effect from individual difference.

11 As previously described [42], primary keratinocytes were cultured in Keratinocyte Basal Medium

12 (KBM, Lonza #CC-4131) supplemented with 100 U/mL Penicillin/Streptomycin (Gibco Life Technology

13 #15140122), 0.1 mM ethanolamine (Sigma Aldrich #141-43-5), 0.1 mM O-phosphoethanolamine

14 (Sigma Aldrich #1071-23-4), 0.4% (vol/vol) bovine pituitary extract, 0.5 μg/mL hydrocortisone, 5

15 μg/mL insulin and 10 ng/mL epidermal growth factor (Lonza #CC-4131). Medium was refreshed

16 every other day. When cells were more than 90% confluent, cells were collected at the proliferation

17 stage. No mycoplasma contamination is found during cell culture.

18 **ATAC-seq**

19 ATAC libraries of the control and p63 mutant keratinocytes were prepared by a documented

20 protocol [43]. In brief, keratinocytes were treated with Accutase® solution on plates and well re-

21 suspended into single cells. Pellet cells for 5 min at 500 g. After twice wash with ice-old PBS, pellet

22 the cells again. Re-suspend cells and take out 100,000 cells for lysis with ice-old freshly made lysis

23 buffer (containing 10 mM Tris-HCl pH 7.5, 10 mM NaCl, 3 mM $MgCl_2$ and 0.1% IGEPAL CA-630

24 detergent). Then perform tagmentation using 2 μl of Tn5 transposase and 12.5 ul 2 × TD buffer

25 (Illumina #FC-121-1031) at 37°C for 1h with 650 rpm shaking. The resulted DNA fragments

26 underwent two sequential seven-cycle PCR amplification, and in between the libraries were selected

27 for <500 bp fragments using SPRI beads. The final PCR products were purified with QIAquick PCR

28 Purification Kit (QIAGEN #28106) and quantified with the KAPA Library Quantification Kit (Kapa

29 Biosystems #KK4844), and then sequenced in a paired-ended manner using the NextSeq 500

30 (Illumina) according to standard Illumina protocols.

31 **CTCF ChIP-seq**

1   Chromatin for ChIP was prepared as previously described [20]. ChIP assays were performed

2   following a standard protocol [44] with minor modifications. On average, 0.5M keratinocytes were

3   used in each ChIP. 4x ChIP reactions are pooled to prepare one ChIP-seq sample. Antibodies against

4   CTCF (Millipore #07-729, 5ul) was used in each ChIP assay. Resulted DNA fragments from four

5   independent ChIP assays were purified with QIAquick PCR Purification Kit (QIAGEN #28106).

6   Afterwards, 5 ng DNA fragments were pooled and proceeded on with library construction using

7   KAPA Hyper Prep Kit (Kapa Biosystems #KK8504) according to the standard protocol. The prepared

8   libraries were then sequenced using the NextSeq 500 (Illumina) according to standard Illumina

9   protocols.

10   **RNA-seq data analysis**

11   Paired-end RNA-seq reads were mapped to the human genome hg19 using STAR aligner[45] in two-

12   pass mode with default parameters, and enumerate stranded gene-level read counts at the same

13   time. The generated count matrix was used as input for DESeq2 package [46] to distinguish

14   differential expressed genes between control and mutant keratinocytes. These genes greater than

15   1.5-fold changed at adjusted p value < 0.05 were considered significantly deregulated.

16   **ChIP-seq and ATAC-seq data analysis**

17   Sequenced reads were aligned against the UCSC hg19 human reference genome with Burrows-

18   Wheeler Aligner (BWA) program with default parameters [47]. The potential PCR and optical

19   duplicates were removed using Picard *MarkDuplicates* option. The filtered BAM files were inputted

20   to MACS2 [48] for peak calling. The p63 ChIP-seq data was published and re-analyzed in this study

21   [13]. The p63, CTCF and H3K27ac were called using the narrow setting (default) with a q-value of

22   0.01. For ATAC-seq, the open chromatin regions were predicted using default parameters except for

23   using -f BAMPE option. Peaks overlapping with the consensus excludable ENCODE blacklist were

24   dropped to avoid confounding by repetitive regions. All alignment files were extended to 200-bp and

25   scaled to RPKM-normalized read coverage files using deepTools [49] for visualization. To compare

26   binding profiles between different samples unbiasedly, we applied library size factors estimated

27   from DESeq2 [46] on RPKM values.

28   Differentially accessible regions were detected using DESeq2 package [46] with fold change less than

29   2.0 and p-value below 0.05. Differential motif analysis in the differential DHSs was employed by the

30   findMotifs function in HOMER tool (http://homer.salk.edu/homer/motif/) with other default

31   parameters, which can normalize the background sequences to remove GC-bias. The BEDtools suite

1   (https://bedtools.readthedocs.io/en/latest/content/bedtools-suite.html) was used to test overlap

2   and enrichment between different intervals.

3   **Dimensionality reduction and functional annotation**

4   For visualization, top 1,000 variable genes were first selected based on interquartile range (IQR) of

5   normalized expression values, and further used to reduce dimensionality (principal component

6   analysis) of the dataset by pca function in R. Functional enrichment was evaluated by Metascape

7   online tool [50], to gain insight into the biological functions for deregulated genes. Only these

8   functional terms with Benjamini-adjusted p-value < 0.05 were considered significantly

9   overrepresented.

10   **Capture Hi-C data processing**

11   Raw Promoter Capture Hi-C sequencing reads from GSE84662 were processed using the HiCUP

12   pipeline [51], like quality control, alignment to hg19 and reads filtering. Technical replicates were

13   merged and de-duplicated, and then pooled biological replicates was then jointly used for

14   interaction identification with CHiCAGO [52] and the associated chicagoTools suite. All significant

15   interactions were defined based on a strict interaction threshold (CHiCAGO score $\geqslant$ 5).

16   Briefly, CHiCAGO predicts interactions based on a convolution background model reflecting both

17   'Brownian' (real, but expected interactions) and 'technical' (assay and sequencing artifacts)

18   components. The putative p values are corrected using a weighted false discovery control procedure

19   that specifically accommodates the fact that increasingly larger numbers of tests are performed at

20   regions where progressively smaller numbers of interactions are expected. The weights were

21   learned based on the decrease of the reproducibility of interaction calls between the individual

22   replicates of macrophage samples with distance. Interaction scores were then computed for each

23   fragment pair as –log-transformed, soft-thresholded, weighted p values.

24

25

26

Author Contributions

JQ, GY and HZ conceived and designed the experiments. JQ, GY, HZ wrote and revised the manuscript. JQ performed the experiments. JQ, GY and HZ analysed the data.

Acknowledgements

We thank Eva Janssen-Megens, Siebe van Genesen and Rita Bylsma for operating the Illumina analyzer. We thank the ENCODE Consortium for sharing their data.

Competing interests

None of the authors have any competing interests in the manuscript.

Data availability

To review our complete dataset GEO accession GSE123711 (https://www.ncbi.nlm.nih.gov/geo/query/acc.cgi?acc=GSE123711). All data supporting the findings of the study and in-house codes are available on request.

Ethics approval and consent to participate

Not applicable.

Declarations:

Consent for publication

Not applicable.

Funding

References

1. Truong AB, Kretz M, Ridky TW, Kimmel R, Khavari PA: **p63 regulates proliferation and differentiation of developmentally mature keratinocytes**. *Genes Dev* 2006, **20**(22):3185-3197.

2. Lippens S, Denecker G, Ovaere P, Vandenabeele P, Declercq W: **Death penalty for keratinocytes: apoptosis versus cornification**. *Cell death and differentiation* 2005, **12**(S2):1497.

3. Botchkarev VA, Flores ER: **p53/p63/p73 in the epidermis in health and disease**. *Cold Spring Harbor perspectives in medicine* 2014, **4**(8):a015248.

4. Kouwenhoven EN, Oti M, Niehues H, van Heeringen SJ, Schalkwijk J, Stunnenberg HG, van Bokhoven H, Zhou H: **Transcription factor p63 bookmarks and regulates dynamic enhancers during epidermal differentiation**. *EMBO Rep* 2015, **16**(7):863-878.

5. Bao X, Rubin AJ, Qu K, Zhang J, Giresi PG, Chang HY, Khavari PA: **A novel ATAC-seq approach reveals lineage-specific reinforcement of the open chromatin landscape via cooperation between BAF and p63**. *Genome Biol* 2015, **16**(1):284.

6. LeBoeuf M, Terrell A, Trivedi S, Sinha S, Epstein JA, Olson EN, Morrisey EE, Millar SE: **Hdac1 and Hdac2 act redundantly to control p63 and p53 functions in epidermal progenitor cells**. *Dev Cell* 2010, **19**(6):807-818.

7. Koster MI, Dai D, Marinari B, Sano Y, Costanzo A, Karin M, Roop DR: **p63 induces key target genes required for epidermal morphogenesis**. *Proceedings of the National Academy of Sciences* 2007, **104**(9):3255-3260.

8. Romano R-A, Ortt K, Birkaya B, Smalley K, Sinha S: **An active role of the ΔN isoform of p63 in regulating basal keratin genes K5 and K14 and directing epidermal cell fate**. *PloS one* 2009, **4**(5):e5623.

9. Fessing MY, Mardaryev AN, Gdula MR, Sharov AA, Sharova TY, Rapisarda V, Gordon KB, Smorodchenko AD, Poterlowicz K, Ferone G *et al*: **p63 regulates Satb1 to control tissue-specific chromatin remodeling during development of the epidermis**. *J Cell Biol* 2011, **194**(6):825-839.

10. Mardaryev AN, Gdula MR, Yarker JL, Emelianov VU, Poterlowicz K, Sharov AA, Sharova TY, Scarpa JA, Joffe B, Solovei I *et al*: **p63 and Brg1 control developmentally regulated higher-order chromatin remodelling at the epidermal differentiation complex locus in epidermal progenitor cells**. *Development* 2014, **141**(1):101-111.

11. Keyes WM, Pecoraro M, Aranda V, Vernersson-Lindahl E, Li W, Vogel H, Guo X, Garcia EL, Michurina TV, Enikolopov G: **ΔNp63α is an oncogene that targets chromatin remodeler Lsh to drive skin stem cell proliferation and tumorigenesis**. *Cell stem cell* 2011, **8**(2):164-176.

12. Rinaldi L, Datta D, Serrat J, Morey L, Solanas G, Avgustinova A, Blanco E, Pons JI, Matallanas D, Von Kriegsheim A *et al*: **Dnmt3a and Dnmt3b Associate with Enhancers to Regulate Human Epidermal Stem Cell Homeostasis**. *Cell Stem Cell* 2016, **19**(4):491-501.

13. Qu J, Tanis S, Smits J, Kouwenhoven EN, Oti M, Logie C, Stunnenberg H, Mulder K, Zhou H: **Mutant p63 affects epidermal cell identity through rewiring the enhancer landscape**. 2018.

14. Rinne T, Brunner HG, van Bokhoven H: **p63-associated disorders**. *Cell Cycle* 2007, **6**(3):262-268.

15. Rinne T, Hamel B, Bokhoven Hv, Brunner HG: **Pattern of p63 mutations and their phenotypes—update**. *American Journal of Medical Genetics Part A* 2006, **140**(13):1396-1406.

16. Ong C-T, Corces VG: **CTCF: an architectural protein bridging genome topology and function**. *Nature reviews Genetics* 2014, **15**(4):234.

17. Kundaje A, Meuleman W, Ernst J, Bilenky M, Yen A, Heravi-Moussavi A, Kheradpour P, Zhang Z, Wang J, Ziller MJ: **Integrative analysis of 111 reference human epigenomes**. *Nature* 2015, **518**(7539):317.

18. Rubin AJ, Barajas BC, Furlan-Magaril M, Lopez-Pajares V, Mumbach MR, Howard I, Kim DS, Boxer LD, Cairns J, Spivakov M: **Lineage-specific dynamic and pre-established enhancer–**

promoter contacts cooperate in terminal differentiation. *Nature genetics* 2017, **49**(10):1522.

19. Phanstiel DH, Van Bortle K, Spacek D, Hess GT, Shamim MS, Machol I, Love MI, Aiden EL, Bassik MC, Snyder MP: **Static and dynamic DNA loops form AP-1-bound activation hubs during macrophage development**. *Molecular cell* 2017, **67**(6):1037-1048. e1036.

20. Kouwenhoven EN, van Heeringen SJ, Tena JJ, Oti M, Dutilh BE, Alonso ME, de la Calle-Mustienes E, Smeenk L, Rinne T, Parsaulian L *et al*: **Genome-Wide Profiling of p63 DNA-Binding Sites Identifies an Element that Regulates Gene Expression during Limb Development in the 7q21 SHFM1 Locus**. *PLoS Genet* 2010, **6**(8).

21. Vigano MA, Lamartine J, Testoni B, Merico D, Alotto D, Castagnoli C, Robert A, Candi E, Melino G, Gidrol X *et al*: **New p63 targets in keratinocytes identified by a genome-wide approach**. *Embo J* 2006, **25**(21):5105-5116.

22. McDade SS, Henry AE, Pivato GP, Kozarewa I, Mitsopoulos C, Fenwick K, Assiotis I, Hakas J, Zvelebil M, Orr N *et al*: **Genome-wide analysis of p63 binding sites identifies AP-2 factors as co-regulators of epidermal differentiation**. *Nucleic Acids Res* 2012, **40**(15):7190-7206.

23. Sethi I, Sinha S, Buck MJ: **Role of chromatin and transcriptional co-regulators in mediating p63-genome interactions in keratinocytes**. *BMC Genomics* 2014, **15**:1042.

24. Cavazza A, Miccio A, Romano O, Petiti L, Malagoli Tagliazucchi G, Peano C, Severgnini M, Rizzi E, De Bellis G, Bicciato S *et al*: **Dynamic Transcriptional and Epigenetic Regulation of Human Epidermal Keratinocyte Differentiation**. *Stem Cell Reports* 2016, **6**(4):618-632.

25. Fan X, Wang D, Burgmaier JE, Teng Y, Romano R-A, Sinha S, Yi R: **Single Cell and Open Chromatin Analysis Reveals Molecular Origin of Epidermal Cells of the Skin**. *Developmental cell* 2018.

26. Soares E, Xu Q, Li Q, Qu J, Zheng Y, Raeven HHM, Brandao K, van den Akker WMR, Tang F, Zhou H: **Single-cell RNA-seq identifies a reversible epithelial-mesenchymal transition in abnormally specified epithelia of p63 EEC syndrome**. *bioRxiv* 2018.

27. Yang A, Zhu Z, Kapranov P, McKeon F, Church GM, Gingeras TR, Struhl K: **Relationships between p63 binding, DNA sequence, transcription activity, and biological function in human cells**. *Mol Cell* 2006, **24**(4):593-602.

28. Kouwenhoven EN, van Bokhoven H, Zhou H: **Gene regulatory mechanisms orchestrated by p63 in epithelial development and related disorders**. *Biochim Biophys Acta* 2015, **1849**(6):590-600.

29. Schwalie PC, Ward MC, Cain CE, Faure AJ, Gilad Y, Odom DT, Flicek P: **Co-binding by YY1 identifies the transcriptionally active, highly conserved set of CTCF-bound regions in primate genomes**. *Genome biology* 2013, **14**(12):R148.

30. Beagan JA, Duong MT, Titus KR, Zhou L, Cao Z, Ma J, Lachanski CV, Gillis DR, Phillips-Cremins JE: **YY1 and CTCF orchestrate a 3D chromatin looping switch during early neural lineage commitment**. *Genome research* 2017.

31. Chernukhin I, Shamsuddin S, Kang SY, Bergström R, Kwon Y-W, Yu W, Whitehead J, Mukhopadhyay R, Docquier F, Farrar D: **CTCF interacts with and recruits the largest subunit of RNA polymerase II to CTCF target sites genome-wide**. *Molecular and cellular biology* 2007, **27**(5):1631-1648.

32. Wendt KS, Grosveld FG: **Transcription in the context of the 3D nucleus**. *Current opinion in genetics & development* 2014, **25**:62-67.

33. Fullwood MJ, Wei C-L, Liu ET, Ruan Y: **Next-generation DNA sequencing of paired-end tags (PET) for transcriptome and genome analyses**. *Genome research* 2009, **19**(4):521-532.

34. Mumbach MR, Rubin AJ, Flynn RA, Dai C, Khavari PA, Greenleaf WJ, Chang HY: **HiChIP: efficient and sensitive analysis of protein-directed genome architecture**. *Nature methods* 2016, **13**(11):919.

35. Jin F, Li Y, Dixon JR, Selvaraj S, Ye Z, Lee AY, Yen C-A, Schmitt AD, Espinoza CA, Ren B: **A high-resolution map of the three-dimensional chromatin interactome in human cells**. *Nature* 2013, **503**(7475):290.

36. Browne G, Cipollone R, Lena AM, Serra V, Zhou H, van Bokhoven H, Dotsch V, Merico D, Mantovani R, Terrinoni A *et al*: **Differential altered stability and transcriptional activity of DeltaNp63 mutants in distinct ectodermal dysplasias**. *J Cell Sci* 2011, **124**(Pt 13):2200-2207.

37. Celli J, Duijf P, Hamel BC, Bamshad M, Kramer B, Smits AP, Newbury-Ecob R, Hennekam RC, Van Buggenhout G, van Haeringen A *et al*: **Heterozygous germline mutations in the p53 homolog p63 are the cause of EEC syndrome**. *Cell* 1999, **99**(2):143-153.

38. Hong J-W, Hendrix DA, Levine MS: **Shadow enhancers as a source of evolutionary novelty**. *Science* 2008, **321**(5894):1314-1314.

39. Barolo S: **Shadow enhancers: Frequently asked questions about distributed cis‐regulatory information and enhancer redundancy**. *Bioessays* 2012, **34**(2):135-141.

40. van Bokhoven H, Hamel BC, Bamshad M, Sangiorgi E, Gurrieri F, Duijf PH, Vanmolkot KR, van Beusekom E, van Beersum SE, Celli J *et al*: **p63 Gene mutations in eec syndrome, limb-mammary syndrome, and isolated split hand-split foot malformation suggest a genotype-phenotype correlation**. *Am J Hum Genet* 2001, **69**(3):481-492.

41. Rheinwald JG, Green H: **Epidermal growth factor and the multiplication of cultured human epidermal keratinocytes**. *Nature* 1977, **265**(5593):421-424.

42. Rinne T, Clements SE, Lamme E, Duijf PH, Bolat E, Meijer R, Scheffer H, Rosser E, Tan TY, McGrath JA *et al*: **A novel translation re-initiation mechanism for the p63 gene revealed by amino-terminal truncating mutations in Rapp-Hodgkin/Hay-Wells-like syndromes**. *Hum Mol Genet* 2008, **17**(13):1968-1977.

43. Liu NQ, Ter Huurne M, Nguyen LN, Peng T, Wang S-Y, Studd JB, Joshi O, Ongen H, Bramsen JB, Yan J: **The non-coding variant rs1800734 enhances DCLK3 expression through long-range interaction and promotes colorectal cancer progression**. *Nature communications* 2017, **8**:14418.

44. Novakovic B, Habibi E, Wang S-Y, Arts RJ, Davar R, Megchelenbrink W, Kim B, Kuznetsova T, Kox M, Zwaag J: **β-Glucan Reverses the Epigenetic State of LPS-Induced Immunological Tolerance**. *Cell* 2016, **167**(5):1354-1368. e1314.

45. Dobin A, Davis CA, Schlesinger F, Drenkow J, Zaleski C, Jha S, Batut P, Chaisson M, Gingeras TR: **STAR: ultrafast universal RNA-seq aligner**. *Bioinformatics* 2013, **29**(1):15-21.

46. Anders S, Huber W: **Differential expression analysis for sequence count data**. *Genome Biol* 2010, **11**(10):R106.

47. Li H, Durbin R: **Fast and accurate short read alignment with Burrows–Wheeler transform**. *bioinformatics* 2009, **25**(14):1754-1760.

48. Zhang Y, Liu T, Meyer CA, Eeckhoute J, Johnson DS, Bernstein BE, Nussbaum C, Myers RM, Brown M, Li W *et al*: **Model-based Analysis of ChIP-Seq (MACS)**. *Genome Biol* 2008, **9**(9):R137.

49. Ramírez F, Dündar F, Diehl S, Grüning BA, Manke T: **deepTools: a flexible platform for exploring deep-sequencing data**. *Nucleic acids research* 2014, **42**(W1):W187-W191.

50. Tripathi S, Pohl MO, Zhou Y, Rodriguez-Frandsen A, Wang G, Stein DA, Moulton HM, DeJesus P, Che J, Mulder LC: **Meta-and orthogonal integration of influenza "OMICs" data defines a role for UBR4 in virus budding**. *Cell host & microbe* 2015, **18**(6):723-735.

51. Wingett S, Ewels P, Furlan-Magaril M, Nagano T, Schoenfelder S, Fraser P, Andrews S: **HiCUP: pipeline for mapping and processing Hi-C data**. *F1000Research* 2015, **4**.

52. Cairns J, Freire-Pritchett P, Wingett SW, Várnai C, Dimond A, Plagnol V, Zerbino D, Schoenfelder S, Javierre B-M, Osborne C: **CHiCAGO: robust detection of DNA looping interactions in Capture Hi-C data**. *Genome biology* 2016, **17**(1):127.
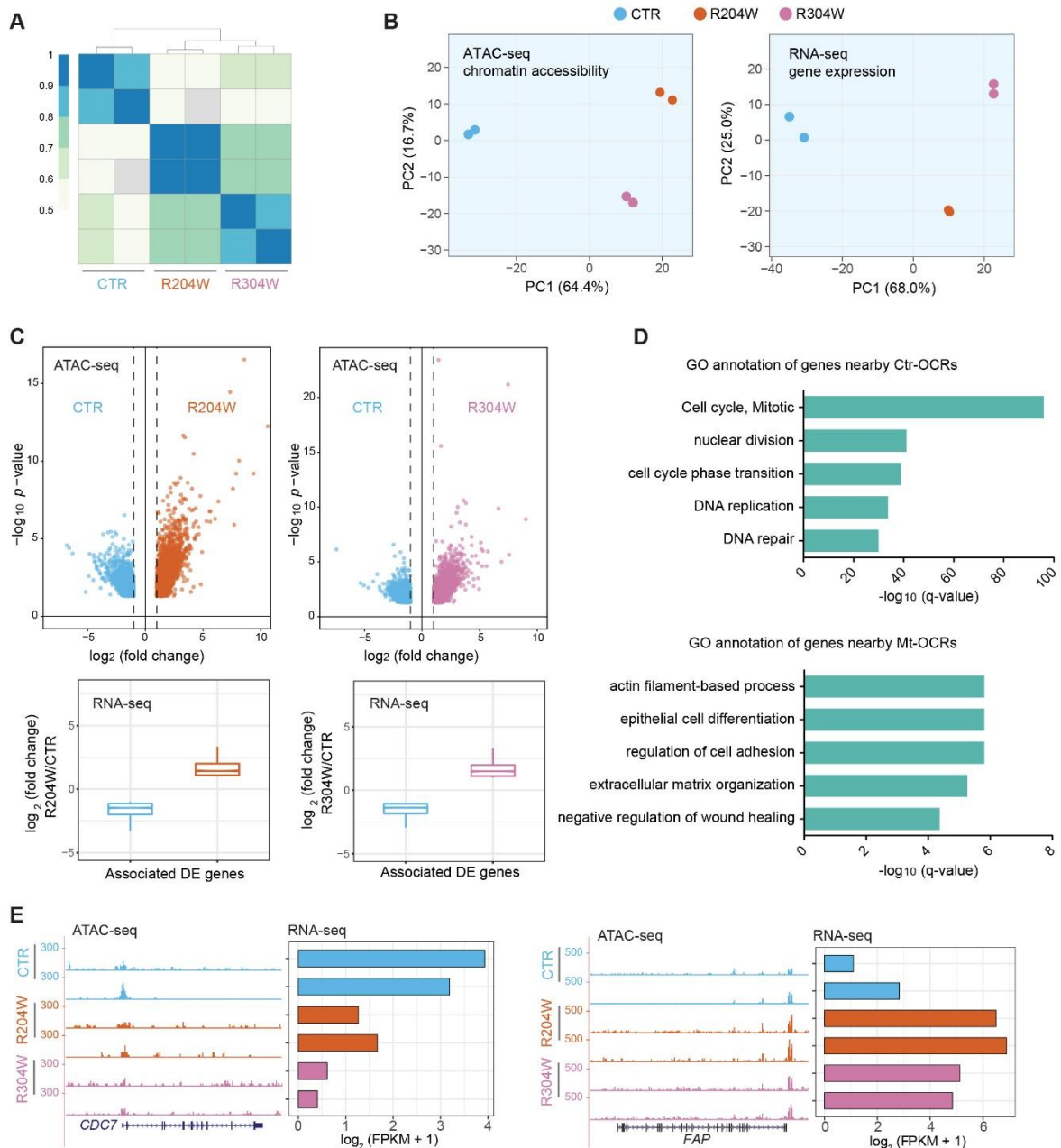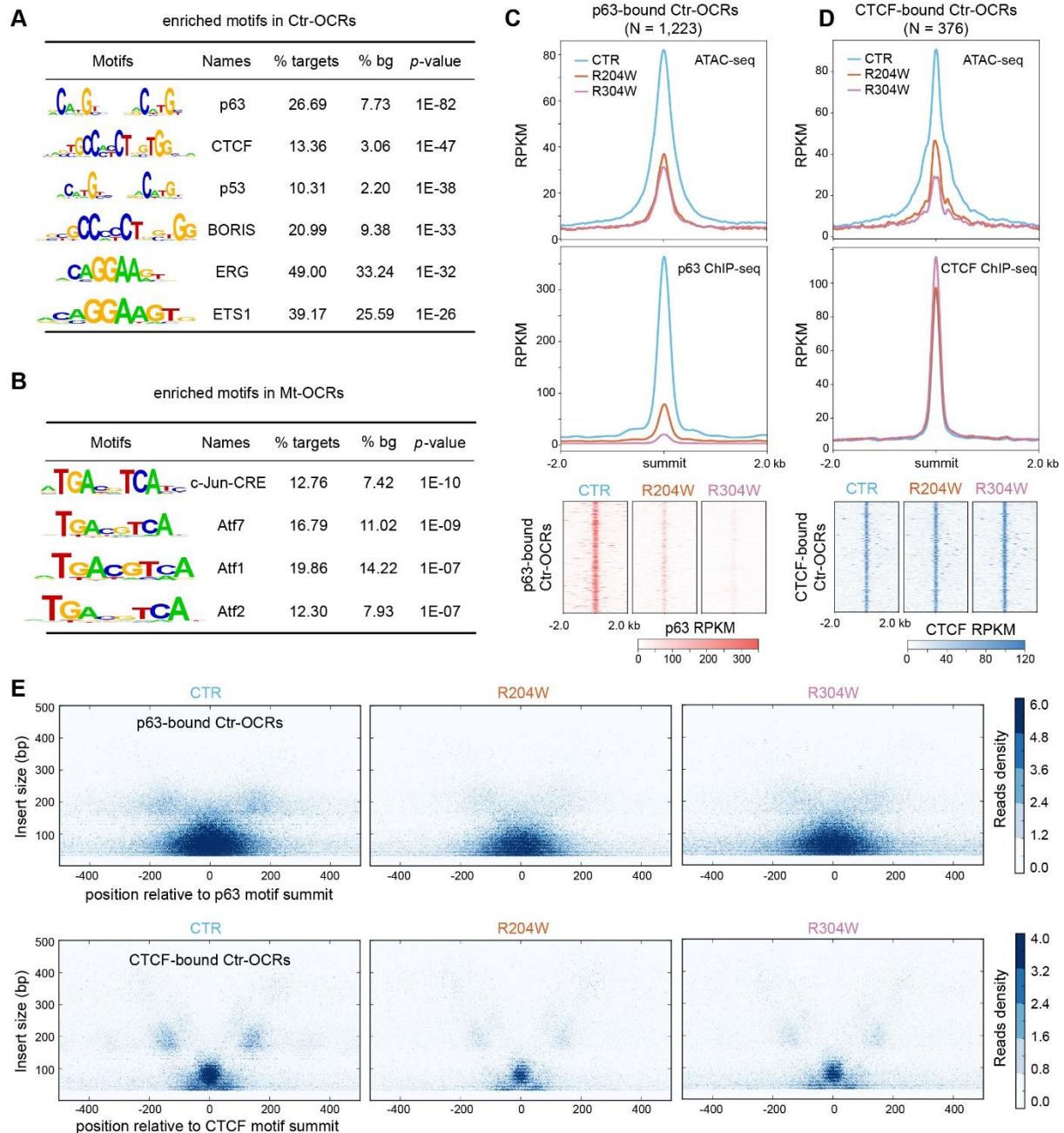
1   **Figures**

2

3   **Figure 1. Differential chromatin accessibility in p63 mutant keratinocytes**

4   A. A heatmap of sample correlation matrix showing high similarities between duplicates and
5   dissimilarities between control (CTR) and p63 mutant keratinocytes (R204W and R304W).

6   B. PCA plots of ATAC-seq and RNA-seq of control and p63 mutant keratinocytes at the
7   proliferation stage.

8   C. Upper panel, volcano plots of ATAC-seq comparisons between control and p63 mutant
9   keratinocytes. The x axis shows the log2 fold change of reads detected at the open
10   chromatin regions (OCRs) and the y axis shows -log10 (p value). Lower panel, the

1   transcriptional changes of differentially expressed genes associated with differential OCRs

2   indicated in the volcano plots.

3   D. GO annotation of differentially expressed genes nearby Ctr-OCRs and Mt-OCRs.

4   E. Examples of Ctr-OCRs and their associated DE gene, *CDC7*, as well as Mt-OCRs and their

5   associated DE gene, *FAP*. ATAC-seq tracks are shown in the RPKM scale.

6

Figure 2. Decreased chromatin accessibility and altered nucleosome organization at p63-bound OCRs and CTCF-bound OCRs in p63 mutant keratinocytes

A. Top enriched motifs in Ctr-OCRs. 2,492 Ctr-OCRs (targets) were used in this analysis with Mt-OCRs as background (bg).

B. Top enriched motifs in Mt-OCRs. 3,716 Mt-OCRs (targets) were used in this analysis with Ctr-OCRs as background (bg).

C. Bandplots (top) and heatmaps (bottom) showing the quantification of ATAC-seq and p63 ChIP-seq signals at the 1,223 p63-bound Ctr-OCRs.

1   D. Bandplots (top) and heatmaps (bottom) showing the quantification of ATAC-seq and CTCF
2   ChIP-seq signals at the 376 CTCF-bound Ctr-OCRs.

3   E. V-plot of ATAC-seq reads showing the read length and distance from either p63 motif (top)
4   or CTCF motif (bottom) in control and p63 mutant keratinocytes. The short fragments (<150
5   bp) were indicative of nucleosome free DNA.
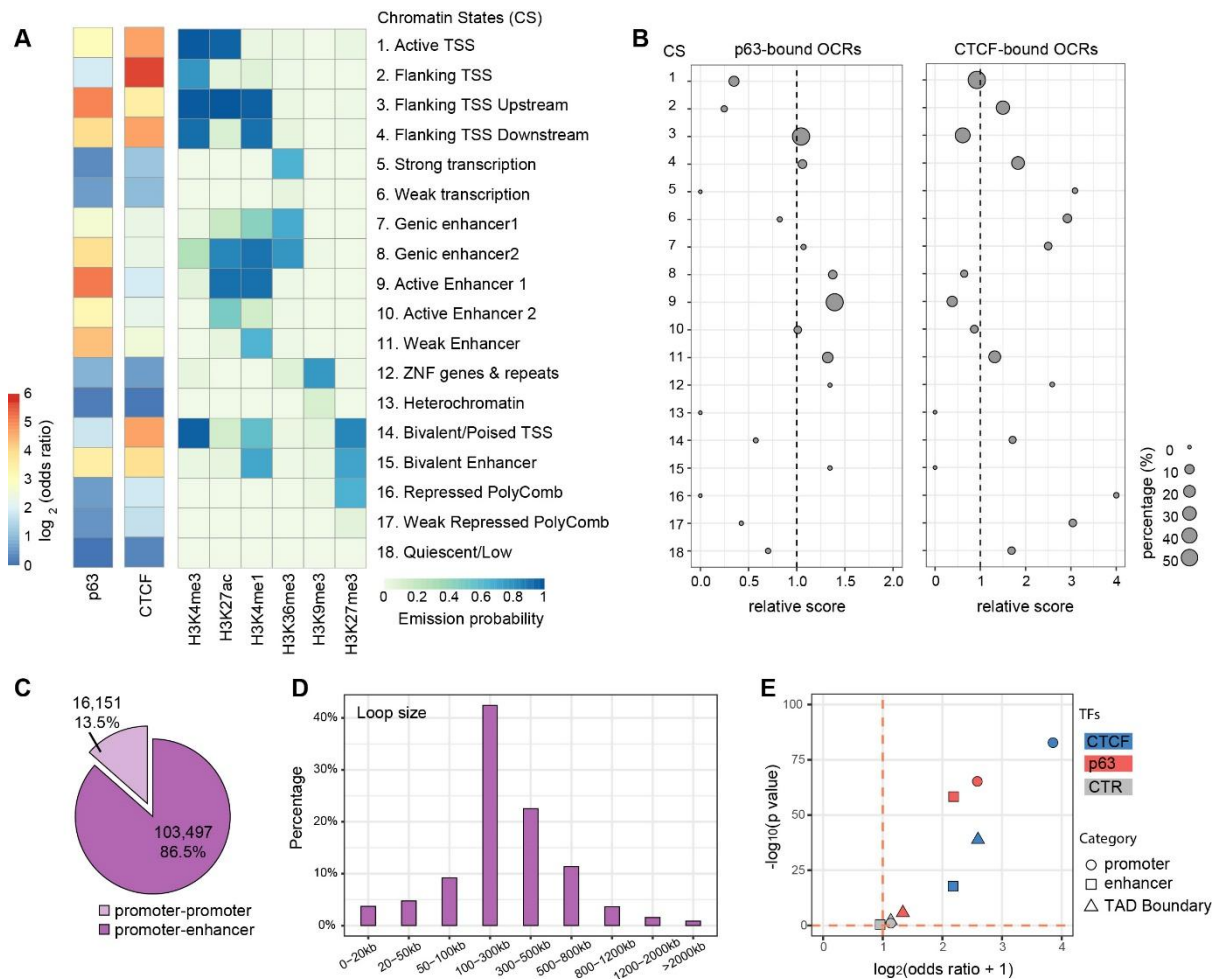
Figure 3. Chromatin state and locations of p63- and CTCF-bound OCRs

A. Fold enrichment/depletion of chromatin states (CSs) in p63 BSs and CTCF BSs compared to the randomized sequences. The 18 CSs were defined using ENCODE data [17].

B. Relative enrichment (> 1)/depletion (< 1) of CSs in p63-bound Ctr-OCRs and CTCF-bound Ctr-OCRs compared to all Ctr-OCRs. The circle size represents the percentage of either p63-bound Ctr-OCRs (left) or CTCF-bound Ctr-OCRs (right) in each CS. Relative score is calculated by comparing odds ratios between two overlap tests, in which odds ratio is estimated by BEDtools *fisher* option.

C. Percentage of different loop types defined in the PCHiC data.

D. Size distribution of promoter-enhancer loops in the PCHiC data.

E. Estimated enrichment of CTCF and p63 at promoters, enhancers, or TAD Boundary compared to the reshuffled sequences (CTR). Odds ratio indicates the enrichment (> 1)/depletion (< 1) of two independent peak lists calculated by BEDtools *fisher* option.
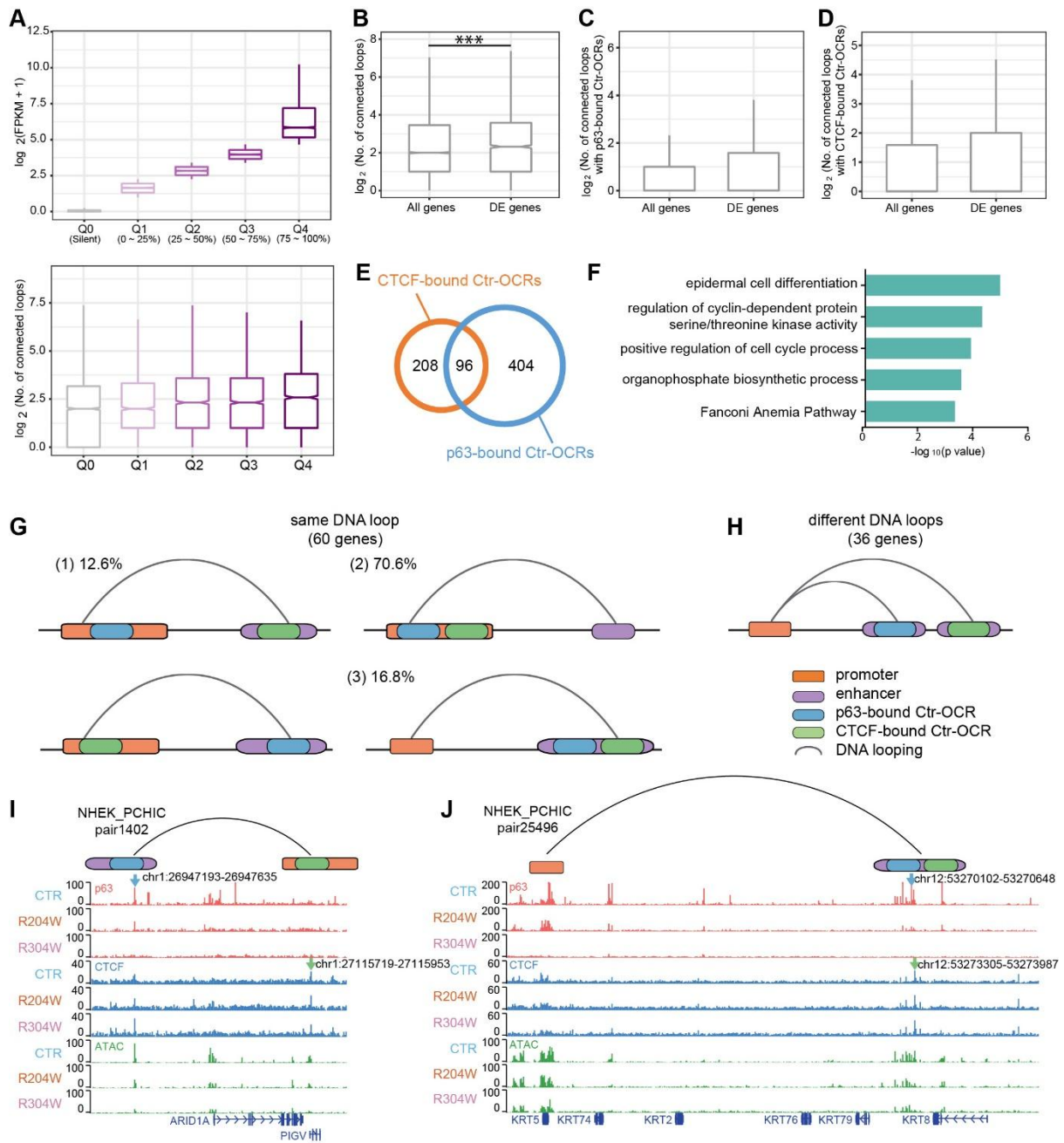
Figure 4. p63- and CTCF-bound Ctr-OCRs are involved in chromatin loops regulating epidermal genes.

A. Highly expressed genes are associated with more DNA loops. Genes were divided in quarters according to their expression levels in keratinocytes. The number of connected DNA loops associated with each group of genes were plotted in the bottom bar chart.

B. DE genes were associated with more connected DNA loops when compared to all expressed genes. ***, $p < 0.001$, Wilcoxon signed-rank test.

C. DE genes were associated with more connected DNA loops with p63-bound Ctr-OCRs when compared to all expressed genes.

D. DE genes were associated with more connected DNA loops with CTCF-bound Ctr-OCRs when compared to all expressed genes.

E. Overlapping of genes mapped by CTCF-bound Ctr-OCRs (orange) and p63-bound Ctr-OCRs (blue).

F. GO annotation of the 96 genes potentially co-regulated by p63 and CTCF.

G. p63-bound and CTCF-bound Ctr-OCRs were involved in the same or different loops connecting the promoters of the 96 genes. 60 genes were regulated by the same loops with both p63-bound and CTCF-bound Ctr-OCRs: (1) in 12.6% cases, p63-bound Ctr-OCR located at one anchor while CTCF-bound Ctr-OCR located at the other anchor of the loop; in the majority cases, p63-bound and CTCF-bound Ctr-OCRs were both present at the (2) promoter (70.6%) or (3) enhancer (16.8%) of the DNA loops.

H. The left 36 genes were co-regulated by connecting DNA loops with p63-bound and CTCF-bound Ctr-OCRs at enhancers of different loops.

I. *PIGV* is shown as an example of G (1), which is connected by the DNA loop pair1402, bridging the PIGV promoter (with a CTCF-bound Ctr-OCR) and a distal enhancer (with a p63-bound Ctr-OCR).

J. *KRT5* is shown as an example of G (3), which is connected by the DNA loop pair25496, bridging the KRT5 promoter and a distal enhancer (with both CTCF-bound and p63-bound Ctr-OCRs). The blue arrows pointed to the p63 BSs while the green arrows pointed to the CTCF BSs.
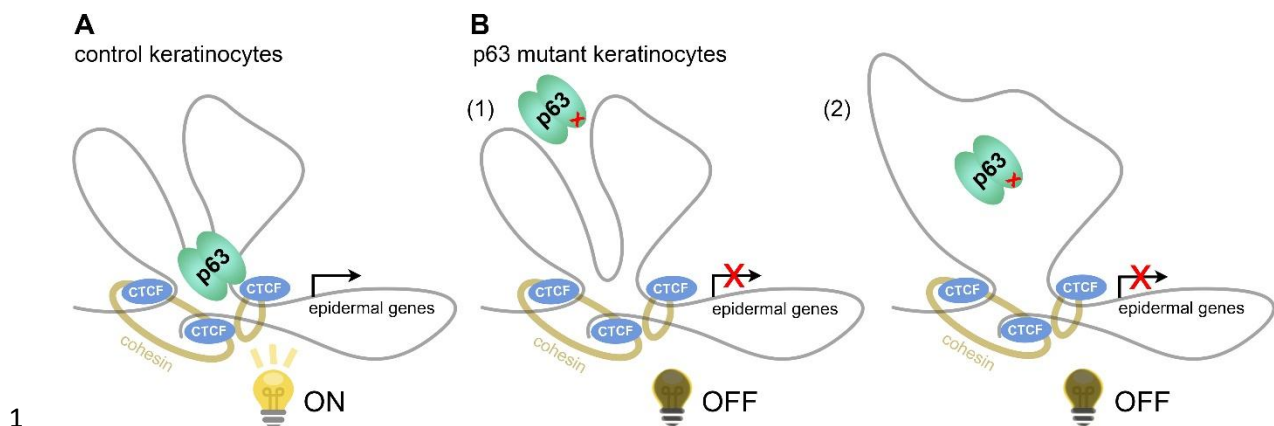
Figure 5. Models of how p63 and CTCF co-mediate chromatin loops regulating epidermal genes.

A. In control keratinocytes, p63 and CTCF co-mediate a subset of DNA loops nearby epidermal genes and regulate their gene expression.

B. In p63 mutant keratinocytes, due to the loss of p63 binding, p63 and CTCF co-mediated DNA loops are not functional anymore, and therefore epidermal genes are deregulated. There are two possibilities in deregulated function of looping: (1) the looping structure is stable as CTCF binding is unchanged; (2) the looping structure is partially changed because of loss of p63 binding and loss of the p63-dependent loop.

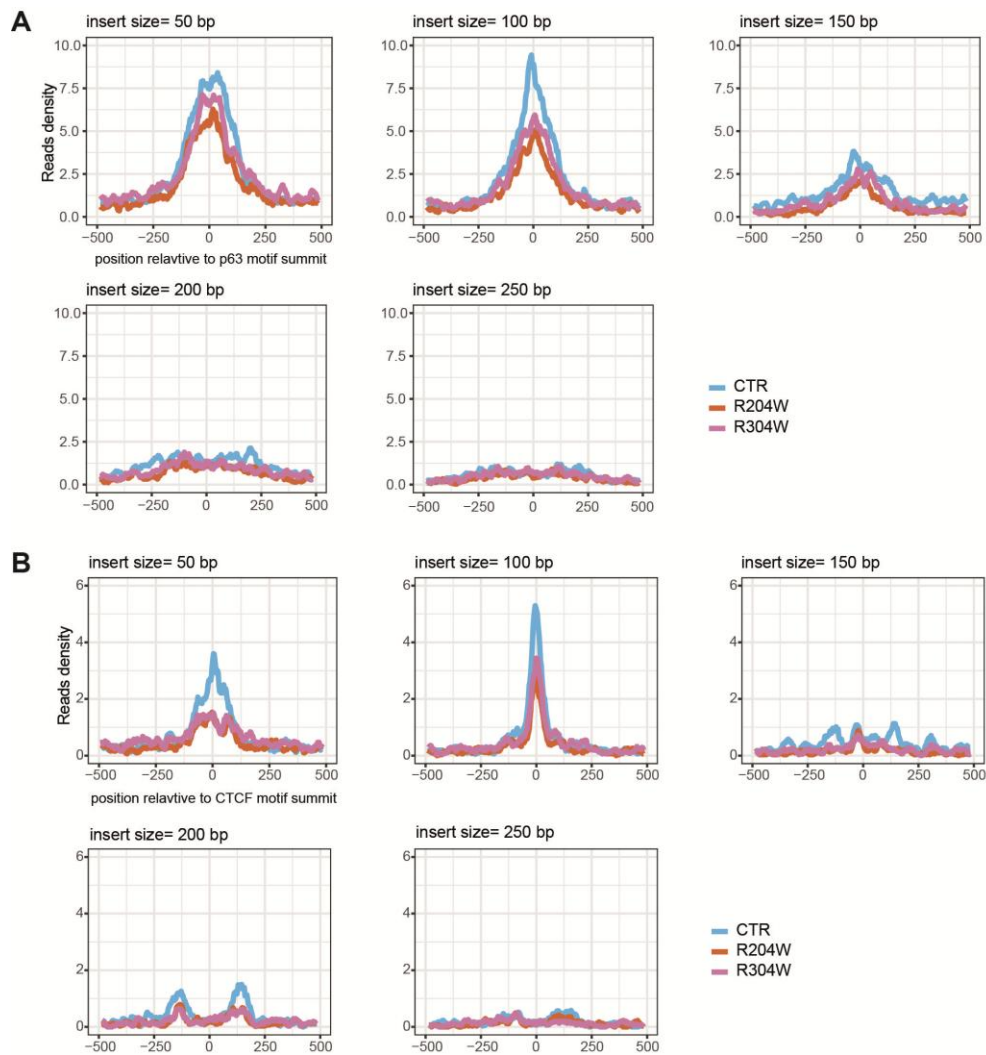1   **Supplementary Figures**
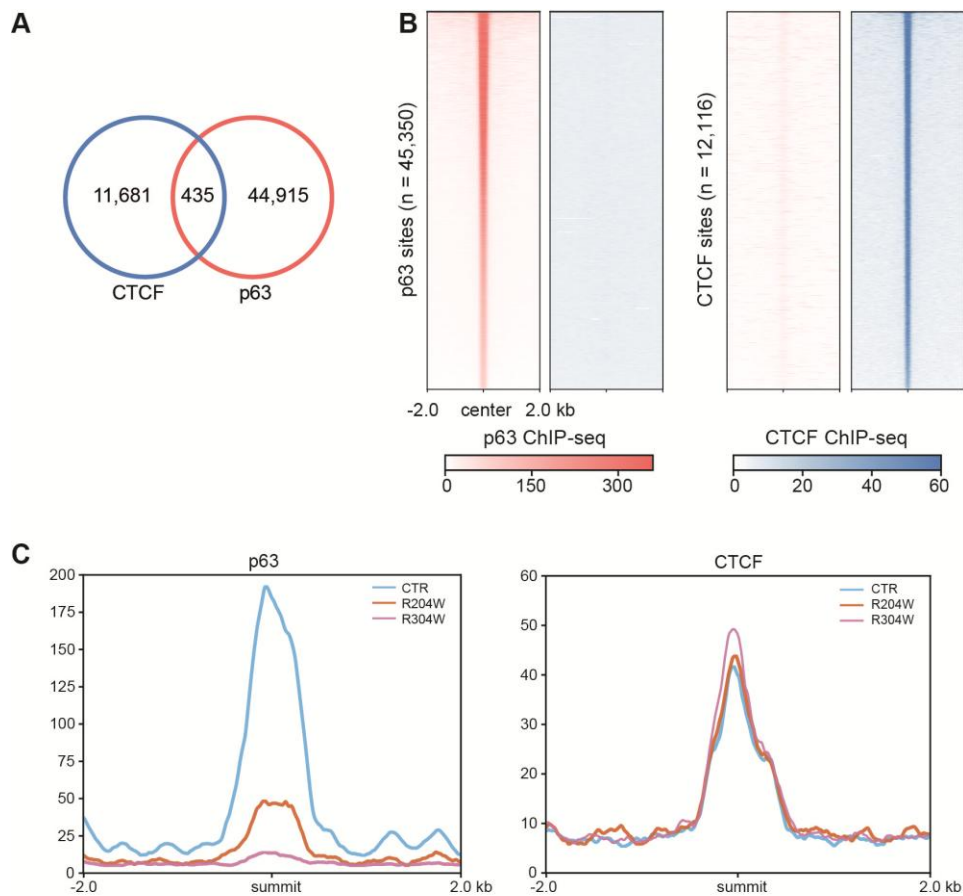
2

3   **Supplementary Figure 1. Few overlap between p63 and CTCF binding sites.**

4   A. Overlapping of p63 and CTCF binding sites from ChIP-seq data

5   B. Heatmaps showing the CTCF binding signal at all 45,350 p63 binding sites (left) and the p63
6   binding signal at all 12,116 CTCF binding sites (right).

7   C. Bandplots showing the p63 binding signal (left) and CTCF binding signal (right) at the 435 co-
8   binding sites in both control and p63 mutant keratinocytes.

9

Supplementary Figure 2. Deregulated nucleosome organization at p63-bound and CTCF-bound Ctr-OCRs in p63 mutant keratinocytes.

D. Reads density of ATAC-seq at p63-bound Ctr-OCRs with different insert sizes in both control and p63 mutant keratinocytes.

E. Reads density of ATAC-seq at CTCF-bound Ctr-OCRs with different insert sizes in both control and p63 mutant keratinocytes.
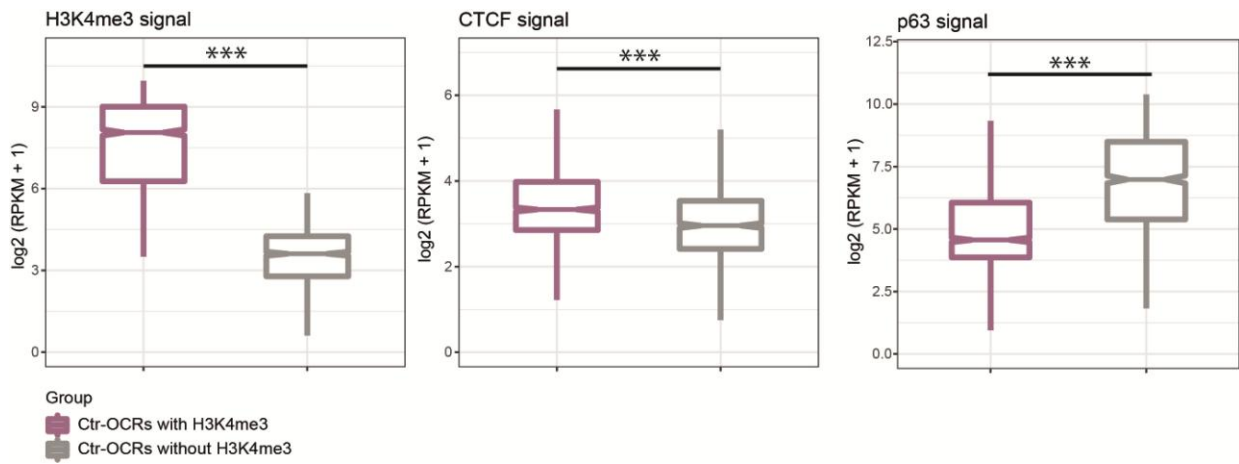
Supplementary Figure 3. CTCF bound preferentially to Ctr-OCRs marked by H3K4me3.

Ctr-OCRs are grouped into two categories according to H3K4me3 signal, Ctr-OCRs with H3K4me3 (purple) and Ctr-OCRs without H3K4me3 (gray). CTCF ChIP-seq showed higher signal in Ctr-OCRs with H3K4me3 while p63 ChIP-seq showed higher signal in Ctr-OCRs without H3K4me3 in control keratinocytes. ***, $p < 0.001$, Wilcoxon signed-rank test.